

More on the QCD phase diagram at finite temperatures

R. V. Gavai

Tata Institute for Fundamental Research, Homi Bhabha Road, Bombay 400005, India

J. Potvin

Physics Department, Boston University, Boston, Massachusetts 02215

and Department of Mathematics, Statistics and Computer Science, Dalhousie University, Halifax, Nova Scotia, Canada B3H 3J5

S. Sanielevici

Physics Department, Brookhaven National Laboratory, Upton, New York 11973

(Received 20 July 1988)

In order to broaden the existing knowledge about the phase diagram of QCD, we use a Langevin algorithm to study finite-temperature QCD on an $8^3 \times 4$ lattice with variable flavor number, quark mass, and gauge coupling. We concentrate on the search for first-order transitions for small flavor number and light-quark masses. We find general agreement with the predictions of effective models of the finite-temperature deconfinement and chiral-symmetry-restoration phase-transition mechanisms. In particular, we find that the deconfinement transition extends to lower quark masses as n_f , the number of quark flavors, decreases. Nonperturbative fermionic effects are found to be significant for very light quarks even for $n_f = 0.1$.

I. INTRODUCTION

The phase diagram of quantum chromodynamics (QCD) at finite temperature has been a subject of intense investigations ever since the early days of numerical simulations of lattice gauge theories. Because of the technical difficulties associated with the proper inclusion of fermions, the first results were obtained in the quenched approximation. These simulations reported indications of discontinuous jumps in various lattice measurables, most notably in the order parameters which characterize confinement and chiral-symmetry breaking.¹ This was interpreted as evidence for a first-order deconfining phase transition, coincident with a first-order chiral-restoration transition.

Subsequently, many analytical² and numerical³ efforts have been directed at extending our understanding of the QCD phase diagram to the full world of interacting dynamical quarks and gluons. Formally, the quenched approximation can be viewed as the limit of QCD in which the quark mass $m \rightarrow \infty$ or the number of dynamically active quark flavors $n_f \rightarrow 0$. Making m finite was the first obvious, computationally not too demanding, step to learn more about the phase diagram. As expected,⁴ one finds⁵ a line of first-order deconfinement phase transitions. The issue of the existence and location of an end point for this line is far from settled,^{5,6} not to mention the problem of determining the nature of this end point.

Meanwhile, attention shifted to very low values of the quark mass, where spontaneous breaking of chiral symmetry at low temperatures and its restoration at finite temperature should be the dominant physics. The results of Gupta *et al.*⁷ indicated the existence of a first-order phase transition in four-flavor QCD with a quark mass of

$ma = 0.025$ in lattice units. Although both the chiral and the deconfinement order parameters showed indications of metastability, as they had in the quenched approximation, these authors labeled this a chiral-symmetry-restoration transition due to the proximity of the chiral limit $m \rightarrow 0$. In fact, this result agrees with analytical and numerical studies of a three-dimensional linear σ model which has been proposed as an effective model of finite-temperature chiral-symmetry restoration.⁸ As summarized in Table I below, the effective model predicts first-order chiral transitions in massless QCD for $n_f \geq 3$. The prediction for $n_f = 2$ depends on whether the effect of the $U_A(1)$ anomaly is suppressed at finite temperature, while no chiral transition is expected for $n_f = 1$.

This paper summarizes the effort which was undertaken by the authors in order to extend the investigations of Ref. 7 to lower flavor number and quark mass, on larger lattices and with better statistics. The main aim was to test the predictions of the effective σ -model analysis, with regard to the existence of first-order phase transitions. We began by verifying the results of Ref. 7 in the four-flavor case, using our own algorithm and methods of data analysis.⁹ We proceeded to study the cases $n_f = 3$ (Ref. 9) and $n_f = 2$ (Ref. 10), as well as the realistic case of a light isodoublet and a heavier strange quark, which interpolates between $n_f = 2$ and 3 (Ref. 11). The main results of these works are included here for completeness, while the emphasis of the presentation is on the results of our new simulations for $n_f = 1$ and 0.1, performed for quark masses between 0.01 and 0.05 (in lattice units) on $8^3 \times 4$ lattices. We interpret this body of results in the light of their relevance to our understanding of the physics of the finite-temperature transition in real-world QCD. Their relationship to the earlier quenched results is discussed. In addition, we address ourselves to more technical ques-

tions such as the utility of approximate algorithms in searching for first-order transitions at low quark masses or the effect of increasing the accuracy of the fermion matrix inversion. Since we have used staggered fermions in our simulations, the comparison of our results to the predictions from the effective model of chiral-symmetry restoration (Ref. 8) can shed light on the validity of the notion of flavors in this fermion scheme.

This paper is organized as follows. In the next section we briefly describe the formalism we used, along with relevant technical remarks. Section III contains a presentation of our results and some conclusions are offered in Sec. IV.

II. FORMALISM

The thermodynamics of QCD can be obtained from the Euclidean partition function Z , given by

$$Z = \int_{\text{BC}} \prod_{x,\mu} dU_x^\mu \prod_x d\chi(x) d\bar{\chi}(x) \exp(-S_G - S_F), \quad (1)$$

where BC denotes the following boundary conditions along the temporal axis:

$$\begin{aligned} U_{\mathbf{x},0}^\mu &= U_{\mathbf{x},N_\beta}^\mu \quad \forall \mathbf{x}, \mu, \\ \chi(\mathbf{x},0) &= -\chi(\mathbf{x},N_\beta) \quad \forall \mathbf{x}, \\ \bar{\chi}(\mathbf{x},0) &= -\bar{\chi}(\mathbf{x},N_\beta) \quad \forall \mathbf{x}. \end{aligned} \quad (2)$$

All variables satisfy periodic boundary conditions in the spatial directions. $U_x^\mu \in \text{SU}(3)$ denotes a gauge variable associated with a link emerging from lattice site x into the positive μ direction. $\chi(x)$ and $\bar{\chi}(x)$ are one-component spinors associated with the lattice site x . These sites and links form a four-dimensional $N_\sigma^3 \times N_\beta$ lattice with spacing a , whose shortest dimension N_β determines the temperature of the system by $T = 1/N_\beta a$.

The actions S_G and S_F are given by

$$S_G = \beta \sum_{x,\mu < \nu} \left(1 - \frac{1}{3} \text{Re tr} U_x^\mu U_{x+\hat{\mu}}^\nu U_{x+\hat{\nu}}^{\mu\dagger} U_x^{\nu\dagger}\right), \quad (3)$$

where β relates to the SU(3) coupling as $\beta = 6/g^2$, and

$$\begin{aligned} S_F = \frac{1}{2} \sum_{x,\mu} (-1)^{x_1+x_2+\dots+x_{\mu-1}} & [\bar{\chi}(x) U_x^\mu \chi(x+\hat{\mu}) \\ & - \bar{\chi}(x) U_{x-\hat{\mu}}^{\mu\dagger} \chi(x-\hat{\mu})] \\ & + ma \sum_x \bar{\chi}(x) \chi(x), \end{aligned} \quad (4)$$

where ma is the bare current-quark mass in lattice units. In the following we will write $S_F = \bar{\chi}(D+ma)\chi = \bar{\chi}M\chi$ as shorthand for Eq. (4).

It is well known¹² that, for $ma=0$, S_F has a continuous $U(1) \times U(1)$ chiral symmetry for all values of the lattice spacing a . As $a \rightarrow 0$, it has an enlarged $U(4) \times U(4)$ symmetry, suggesting that it represents four continuum flavors. One can check numerically in the scaling region whether this larger chiral symmetry of the continuum theory is indeed restored at finite β . First results in this direction¹³ do show the expected trend. We will therefore raise the fermion determinant, which results from an

explicit integration over χ and $\bar{\chi}$ in Eq. (4), to the power $n_f/4$ in order to simulate $n_f=4, 3, 2, 1$, and 0.1 flavors, respectively:

$$Z = \int_{\text{BC}} \prod_{x,\mu} dU_x^\mu e^{-S_G} \text{Det}^{n_f/4}(D+ma) \quad (5)$$

or, in terms of the determinant of a positive-definite matrix:

$$Z = \int_{\text{BC}} \prod_{x,\mu} dU_x^\mu e^{-S_G} \text{Det}^{n_f/8}(D+ma)(D+ma)^\dagger. \quad (6)$$

This prescription can be justified¹⁴ in the context of perturbation theory and has been widely used for numerical simulations. We are aware of its possible inadequacies, especially in the context of anomalies. Still, it appears to be the best available lattice fermion scheme for studying the chiral-symmetry-restoration transition with arbitrary flavor number. Should our results agree with the predictions from the effective σ model, this prescription would become more credible in a nonperturbative context.

The lattice measurables which we have studied are defined as expectation values with respect to the Z of Eq. (6) of the following operators: the deconfinement order parameter (Polyakov loop or Wilson line)

$$L = \sum_{\mathbf{x}} \text{tr} \prod_{i=1}^{N_\beta} U_{\mathbf{x},i}^4 / N_\sigma^3 N_\beta, \quad (7)$$

the order parameter of chiral symmetry

$$\bar{\Psi}\Psi = n_f \text{Tr}(D+ma)^{-1} / 4N_\sigma^3 N_\beta, \quad (8)$$

and the plaquette or 1×1 Wilson loop

$$P = \frac{1}{3} \sum_{x,\mu < \nu} \text{Re tr} U_x^\mu U_{x+\hat{\mu}}^\nu U_{x+\hat{\nu}}^{\mu\dagger} U_x^{\nu\dagger} / 6N_\sigma^3 N_\beta. \quad (9)$$

In Eq. (7), i runs over the sites in the temperature direction. Tr in Eqs. (7) and (9) denotes trace over the SU(3)-color index while Tr in Eq. (8) denotes trace over both color and lattice sites.

Our simulations were done with a shifted first-order Langevin algorithm. This relates the gauge variables at simulation time τ_{n+1} to those at time τ_n by the updating equation

$$U_\mu(x, \tau_{n+1}) = U_\mu(x, \tau_n) \exp(-if_a T_a), \quad (10)$$

where

$$f_a = \epsilon \left[\partial_a S_G[U] - \frac{n_f}{16} \xi^\dagger A_a[U] \xi \right] + \sqrt{\epsilon} \eta_a \quad (11)$$

with the notation

$$\epsilon = \tau_{n+1} - \tau_n \quad (12)$$

and

$$A_a[U] = M^{\dagger-1}[U] \partial_a (M^\dagger M) M^{-1}[U]. \quad (13)$$

The T^a are the generators of SU(3) in the fundamental representation: they satisfy $\text{tr} T_a T_b = \delta_{ab}/2$. ξ^i and η_a are random Gaussian noise:

$$\begin{aligned} \langle \eta_a \rangle &= 0, \quad \langle \eta_a \eta_b \rangle = 2\delta_{ab}, \\ \langle \xi^i \rangle &= 0, \quad \langle \xi^i \xi^j \rangle = 2\delta^{ij}. \end{aligned} \quad (14)$$

The derivatives ∂_a satisfy the commutation relations $[\partial_a, \partial_b] = if_{abc} \partial_c$.

In the limit $\tau_n \rightarrow \infty$, the first-order Langevin algorithm defined by Eqs. (10)–(14) yields link variables $\{U_x^\mu\}$ which are distributed according to an effective action S_{eff} which differs from S_{QCD} at nonzero ϵ . For small ϵ ,

$$S_{\text{eff}} = S_{\text{QCD}} + \epsilon S_1 + \epsilon^2 S_2 + \dots \quad (15)$$

As explained in Refs. 15 and 16, one can remove part of the $O(\epsilon)$ terms in Eq. (15) by shifting the “couplings” and the field variables as below:

$$\beta \rightarrow \beta(1 + \epsilon C_A/12 - \epsilon C_F), \quad (16)$$

$$n_f \rightarrow n_f(1 + \epsilon C_A/12), \quad (17)$$

$$m \rightarrow m/(1 - \epsilon C_F/4), \quad (18)$$

and

$$U_x^\mu \rightarrow U_x^\mu \exp \left[-i \frac{\epsilon}{4} (\partial_a S_{\text{QCD}}) T_a \right] \quad (19)$$

[$C_A = N$ and $C_F = (N^2 - 1)/2N$ represent the Casimir invariants in the adjoint and fundamental representations of $SU(N)$]. Alternatively, these terms in the systematic error can be removed by using a second-order (Runge-Kutta) discretization scheme.^{15,16}

In the fermion simulation algorithm presented above, there are further systematic error terms of $O(\epsilon)$ which cannot be removed by either of these procedures and which are not irrelevant in the continuum limit.¹⁵ These so-called nonintegrable terms cause the universality class of S_{eff} to be different from that of S_{QCD} . In Ref. 16 we have compared the algorithm described above to a version of the Runge-Kutta algorithm in which the nonintegrable terms had been explicitly removed. We found that differences became noticeable only for rather large values of ϵ . By comparing the results for lattice measurables obtained with the shifted first-order algorithm to those obtained by the exact algorithm of Ref. 17, we concluded¹⁶ that $\epsilon = 0.01$ was a reasonable choice on a 4^4 lattice with four flavors of mass $ma = 0.1$ and $\beta = 4.8$. The nonintegrable terms are quite negligible for this choice. However, the effective step size appeared to increase as the quark mass was decreased, so that systematic errors and even nonintegrable terms might become a problem when simulating very light quarks with $\epsilon = 0.01$. By comparing our results on the phase transition with $n_f = 4$ and $ma = 0.025$ with those obtained by an exact algorithm,⁷ we have found⁹ that the conclusions with respect to the strong first-order nature of this transition agree, while our Langevin algorithm gives a value for the critical β which is higher by about 1%.

Encouraged by this result, we shall assume in the following that our simulations with $\epsilon = 0.01$ are in fact in the same universality class as QCD for all studied parameter values. We shall then use comparisons with predictions from the effective models and with simulations by

other groups to judge the quality of this assumption. Also, to minimize the impact of finite- ϵ errors on our ability to judge the order of phase transitions, we shall avoid basing such judgments on averages of lattice measurables.

In addition to the Langevin step size, our algorithm has one more parameter which is not governed by physics and which needs to be tuned optically. This parameter, r , is a measure of the accuracy to which $M^{-1} = (D + ma)^{-1}$ is computed for use in Eq. (13). We have used the conjugate-gradient method to compute the inverse and thus r provided the stopping condition for the conjugate-gradient iterations. If X denotes $M^{-1}\xi$ in Eq. (13), then we define

$$r = |MX - \xi|. \quad (20)$$

Figure 1 shows a sample result of our attempts to test the sensitivity of our algorithm to the value of r . It displays the evolution of $\text{Re}L$ from a “cold” start (all $U_x^\mu = 1$) and a “hot” start (all link variables random) on a 4^4 lattice at $\beta = 5.47$ as a function of Langevin iterations for $r = 0.2$ and 0.0002 . Here $n_f = 1$ and $ma = 0.0125$, which is one of the smallest quark mass values we used. One sees that, apart from statistical fluctuations, both values of r yield essentially identical results. With both residues, one concludes that the hot and cold starts converge after about 3000 iterations. This suggests that for $ma \geq 0.0125$ a value of $r \approx 0.2$ suffices for determining the order of the phase transition. This observation has great

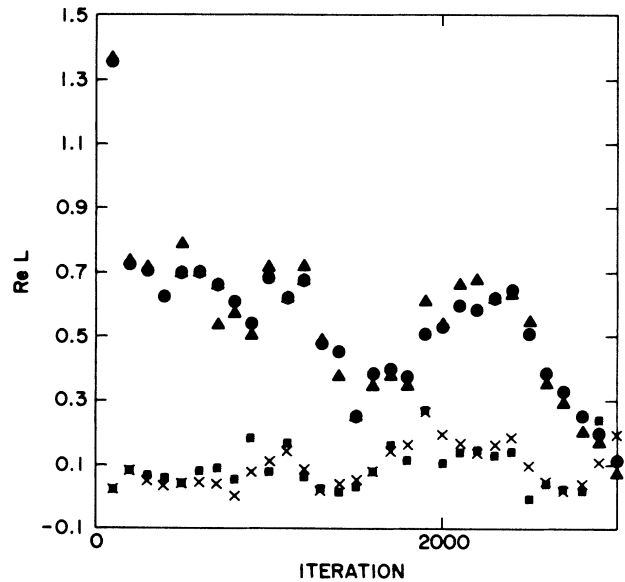


FIG. 1. Effect of a change in the conjugate-gradient inversion residue r [see Eq. (20)] upon the time history of runs from ordered and disordered starts. These sample runs are for $n_f = 1$, $ma = 0.0125$, $\beta = 5.47$ on a 4^4 lattice. Triangles represent the arithmetic mean over 100 iterations of the real part of the Polyakov loop, obtained from an ordered (“cold”) start using $r = 0.2$. Squares represent the disordered (“hot”) start with $r = 0.2$. Circles and crosses depict cold and hot starts, respectively, with $r = 0.0002$.

practical importance, since achieving $r=0.0002$ can require an order of magnitude more computer time than $r=0.2$. In the simulations discussed below, we use $r=0.2$ and 0.1 .

To relate these values of r to the equivalent parameters used by other authors, let us note that $r=0.2$ corresponds to $(r^2/V)^{1/2} \sim 4 \times 10^{-3}$ on a lattice of volume $V=8^3 \times 4$. This is of the order of the inversion stopping parameter values used in Refs. 18–20. When we measure the mean convergence defined in Refs. 7 and 21 on the configurations which give rise to Fig. 1, we typically find $C \sim 10^{-4}$ when $r=0.2$ has been reached, and $C \sim 10^{-9}$ when $r=0.0002$ has been achieved.

Figure 1 also demonstrates the strategy we use to investigate the order of phase transitions. We employed the 4^4 lattice to explore a wide range of β . At each coupling, we made runs from hot and cold starts, as in Fig. 1. Typically after 2000–3000 Langevin iterations, the two runs came together and then evolved similarly irrespective of the start conditions. A lack of convergence over longer runs was interpreted as a possible metastability signal, characteristic of a first-order phase transition. In the narrowed range of β where such behavior occurred, we then reduced the finite-volume effects by increasing the lattice to $8^3 \times 4$. Because of lesser fluctuations on the larger lattice, cleaner metastability signals should be seen if a first-order transition is indeed to occur in the thermodynamic limit.

III. RESULTS

The comparison of the quantitative estimates of the deconfinement temperature in pure SU(3) theory^{3,22} to the preliminary estimates of the transition temperature in QCD with light-quark masses²³ suggests that $T_{\text{SU}(3)} > T_{\text{QCD}}$. This is sketched in Figs. 2(a) and 2(b), where the dashed lines indicate the critical surface spanned by the variables (n_f, m) . Figure 2(c) schematically shows what we may suspect about the nature of this surface. As summarized in Table I, the effective theory of the chiral-restoration transition in massless QCD suggests an n_f -dependent pattern of transitions on the $m=0$ axis of this diagram. On the other hand, the effective theory of the deconfinement transition in pure SU(3) theory predicts a strong first-order phase transition.² This is confirmed by numerical simulations.^{2,3} Since the dynamics in the quenched approximation (along the axes $ma = \infty$ and $n_f = 0$) is identical to that of SU(3), it seems natural to explain the first-order phase transition suggested by simula-

tions done in the quenched approximation¹ as identical to this deconfinement transition. However, the chiral order parameter was also seen to suffer a jump in the quenched simulations. The question arises whether this phenomenon is connected to the chiral-restoration transition. Since Ref. 8 predicts the absence of a first-order chiral transition for $n_f < 2$, an affirmative answer would mean that either Ref. 8 is wrong, or the $n_f \rightarrow 0$ limit of full QCD cannot be taken continuously.

In the effective models of the chiral and deconfinement phase transitions, the fates of these transitions as one moves to finite nonzero masses are predicted on the basis of analogies to spin models in a magnetic field. Finite quark masses act like a magnetic field in the three-dimensional Z_3 effective spin theory of deconfinement; the field increases as the mass becomes lighter.² Similarly, a nonzero quark mass can be represented as a magnetic field term in the effective theory of chiral-symmetry

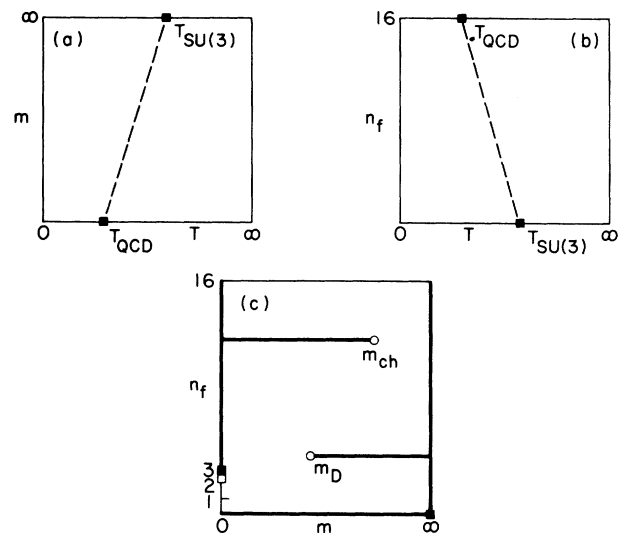


FIG. 2. Sketches of the three-dimensional phase diagram of QCD in the variables (T, m, n_f) , which one expects *before* undertaking a detailed numerical study of the full theory. In (a) and (b), squares denote the first-order phase transitions predicted by effective model studies for pure SU(3) (Refs. 2 and 3) and for massless QCD (Ref. 8). The assumption $T_{\text{SU}(3)} > T_{\text{QCD}}$ is based on Refs. 18 and 19. The dashed lines indicate the surface spanned by flavor number and quark mass, which is sketched in (c). Here, the first-order deconfinement transition of pure SU(3) theory and the predicted chiral-symmetry-restoration transition of massless QCD are indicated by solid squares. Thick lines along the axes at $m = \infty$ and $n_f = 0$ denote the first-order transitions detected in the quenched approximation to QCD (see Refs. 1 and 3). The thick line from $m=0, n_f=3$ to $m=0, n_f=16$ indicates the first-order transitions predicted by Ref. 8; the open square at $m=0, n_f=2$ indicates the ambiguity of the effective model prediction in that case (see Table I). Solid lines stretching into the phase diagram represent the expectation that the first-order chiral and deconfinement transitions should persist for nonzero and finite masses, respectively, ending in points of second-order transitions. The latter are depicted by open circles and labeled m_{ch} and m_{D} , respectively.

TABLE I. Summary of the predictions of Ref. 8 for the order of the chiral-symmetry-restoration phase transition, based on a three-dimensional linear σ model.

$n_f \geq 3$	First order	
$n_f = 2$	First order if weak $U_A(1)$ anomaly for $T \approx T_{\text{ch}}$	Second order with O(4) exponents if $U_A(1)$ anomaly T independent
$n_f = 1$	No chiral transition	

restoration,⁸ the magnitude of this field grows as the mass becomes heavier. The analogy suggests that first-order transitions should weaken gradually while extending into the diagram, eventually terminating in second-order end points. Second-order transitions are not expected to continue into the interior of the phase diagram. Assuming that the quenched first-order transition extends along the axis $n_f=0$, it is not known how it continues into the diagram for finite flavor number at various masses. All this raises the possibility that there could be regions in the surface determined by m and n_f where the low-temperature hadron phase and the high-temperature phase are *not* separated by first-order transitions.

The points raised by such considerations can, at the present time, only be answered by numerical simulations. We have concentrated on the low-mass region for $n_f=0.1, 1, 2, 3$.

$$n_f = 0.1$$

Our chief motivation for studying this case has been a desire to understand the $n_f \rightarrow 0$ limit of QCD, in terms of the relationship between the quenched approximation and massless QCD. Clearly, the place to look for an answer is the limit of very small but nonzero n_f and m . In our formalism, this is easily feasible, although an extrapolation of the flavor interpretation discussed in Sec. II is heavily involved. As we noted above, no effective model predictions are available for this case, so our results will have to be judged in conjunction with the results we shall obtain for larger values of n_f . There is also the issue whether the limit of small n_f can be treated perturbatively.

We searched for first-order phase transitions at three values of the quark mass; $ma=0.05, 0.025$, and 0.01 . On the 4^4 lattice we found indications of possible metastabilities over the following β intervals: $5.60 \leq \beta \leq 5.68$ for $ma=0.05$, $5.56 \leq \beta \leq 5.60$ for $ma=0.025$, and $5.54 \leq \beta \leq 5.58$ for $ma=0.01$. Figures 3 and 4 show our results on the $8^3 \times 4$ lattice for $ma=0.05, \beta=5.64$ and $ma=0.025, \beta=5.58$, respectively. A clear two-state signal is seen in both cases. Although $\text{Re}L$ is plotted here, clear metastability signals are also seen in the other quantities defined in Sec. II, notably in the chiral order parameter. The quality of the two-state signal is comparable to those obtained in the quenched approximation.

As Fig. 5 illustrates, however, no such metastability could be found for $ma=0.01$. Typically after 3000–4000 iterations, the hot and the cold start came together at each of the β that we explored in the above-mentioned range. Thus, there seem to be first-order phase transitions for $ma=0.05$ and 0.025 but not for $ma=0.01$.

A plausible way to understand these results is the following: a line of first-order phase transitions runs from $(n_f=0.1, m=\infty)$ down till $(n_f=0.1, m_D)$, where the second-order end point m_D , predicted by the effective spin model of the pure-gluon deconfinement transition, lies somewhere between $ma=0.01$ and 0.025 (see Fig. 6). Since this line is not connected to the axis $m=0$, it does not seem appropriate to label it a line of chiral transitions. It seems more natural to ascribe the dynamics of

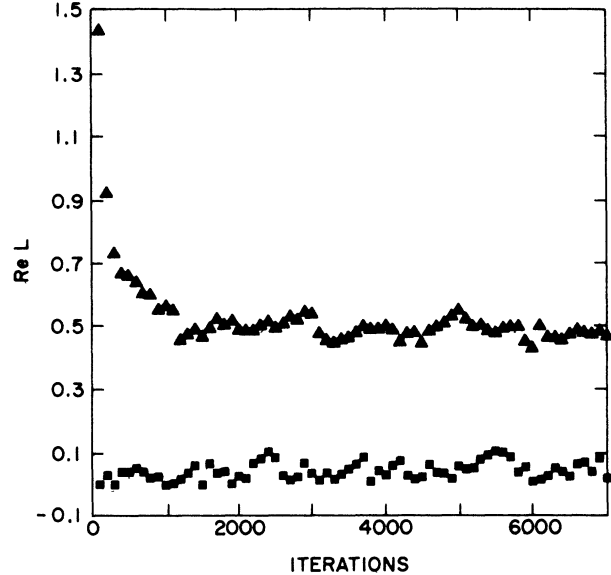


FIG. 3. Time histories from ordered and disordered starts on an $8^3 \times 4$ lattice for $n_f=0.1$, $ma=0.05$, $\beta=5.64$. Triangles represent the arithmetic mean of $\text{Re}L$ over 100 iterations, for the run which proceeded from an ordered (“cold”) start. Squares represent the corresponding run from a disordered (“hot”) start.

these transitions to the deconfinement phenomenon. The jump in $\langle \bar{\Psi}\Psi \rangle$ would thus appear to be induced by the gauge field dynamics. The latter interpretation can also help to understand why jumps occur in the chiral condensate computed with various flavors of static light quarks in a pure SU(3) (dynamical quark mass $m = \infty$) background.

Of course, a first-order chiral transition might appear for still lower values of the quark mass. Also, the first-

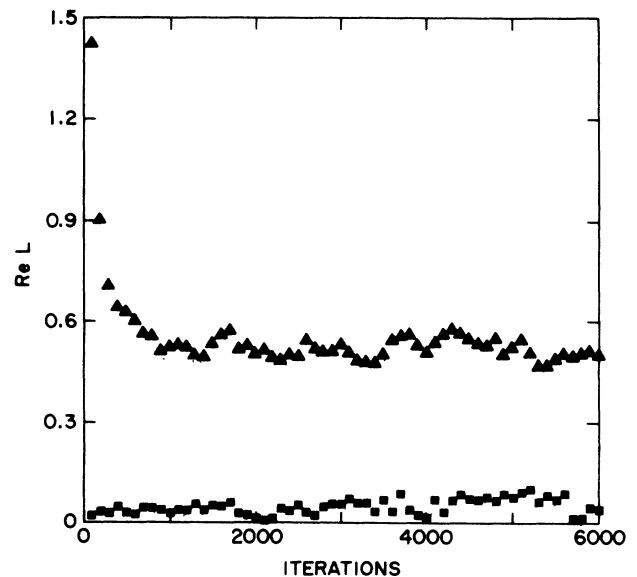


FIG. 4. Same as Fig. 3, but for $n_f=0.1$, $ma=0.025$, $\beta=5.58$.

order line might extend all the way down to $m=0$ for some smaller value $n_f < 0.1$. While the first possibility appears unlikely, mainly in view of our results for $n_f=1$ (see below), the analogy with spin models in a magnetic field would favor the latter conjecture. Indeed, the strength of the fermionic symmetry-breaking field increases proportional to n_f and inversely proportional to some power of m . This statement is, of course, strictly valid only for large quark masses.² Nevertheless, it suggests that the end point m_D should decrease towards lighter and lighter masses as n_f gets smaller. It thus seems possible that in the “completely quenched” case $n_f=0$, perhaps even for some very small but finite n_f , the first-order line would extend all the way between $m=0$ and $m=\infty$. Simulations at still lower values of n_f and

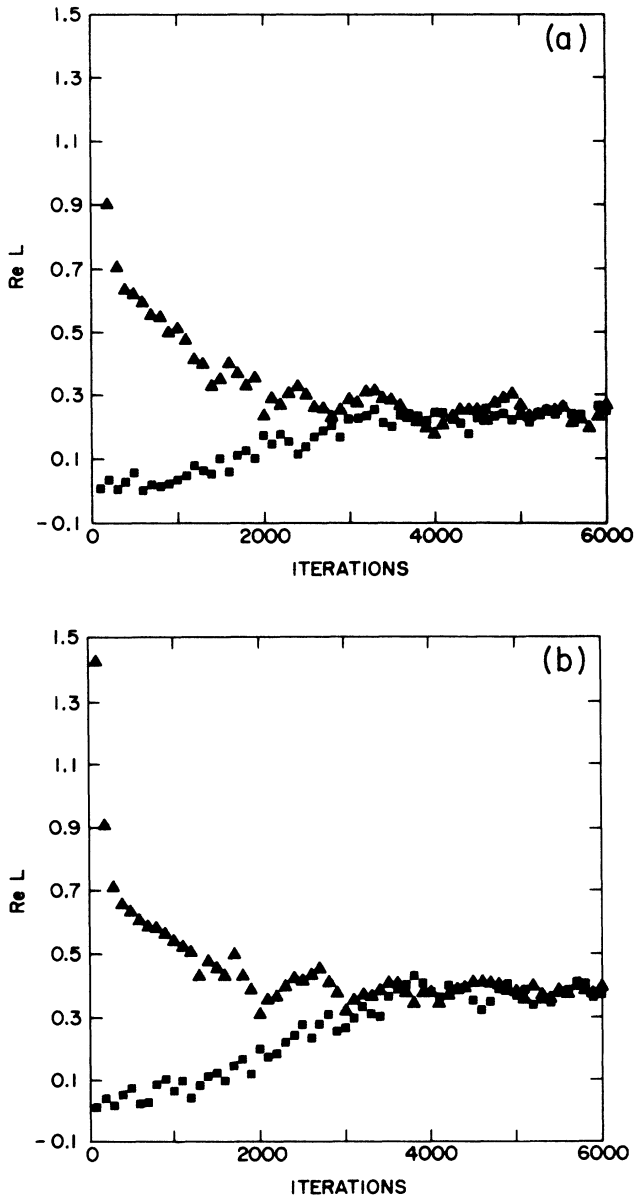


FIG. 5. (a) Same as Fig. 4, but for $n_f=0.1$, $m_a=0.01$, $\beta=5.55$. (b) Same as (a), but for $\beta=5.57$.

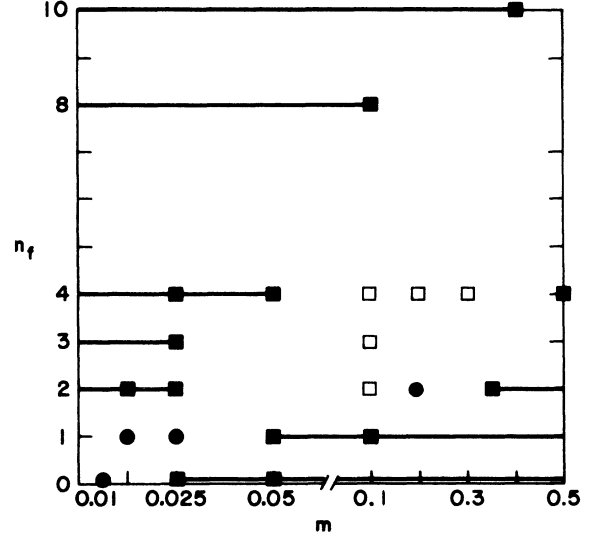


FIG. 6. Status of our present knowledge about the critical surface spanned by quark mass and number of flavors. This is the same surface as sketched in Fig. 2(c), but it now contains the information obtained by numerical simulations of the full theory. Solid squares denote undisputed first-order transitions found in the present work and/or by other authors. These are linked up with the corresponding limit ($m=\infty$ for deconfinement and $m=0$ for chiral restoration) whenever possible, forming the first-order lines suggested by such simulation results. Open squares denote disputed first-order transitions (claimed by some groups but not seen by others). Solid circles show cases in which the present authors have not seen metastability signals and in which there are no contrary claims.

ma would be required to solve such questions conclusively.

It is interesting that the chiral values we obtained for β are clearly distinct from the pure SU(3) value $\beta_c = 5.675$ as measured on an $8^3 \times 4$ lattice.²² Neglecting the dependence on the quark mass and concentrating on the effect of changing the flavor number from zero to $n_f=0.1$, we can estimate the expected shift in the chiral β . Assume (i) that this small change in n_f means essentially no physical change from the quenched approximation, so that the transition temperature in MeV remains the same, and (ii) that the QCD Λ parameters are equal in both cases: $\Lambda(n_f=0.1) = \Lambda(n_f=0)$. Denoting $\beta = \beta(n_f=0)$, the shift $\Delta\beta = \beta - \beta(n_f=0.1)$ is given by

$$\Delta\beta = \frac{0.0061\beta + 0.00017 \ln 2.39\beta - 0.00212}{1 - 0.8427/\beta}, \quad (21)$$

where we have used the usual two-loop renormalization-group formula. Substituting $\beta = 5.675$, we get $\Delta\beta = 0.039$. This is to be compared with the observed values $\Delta\beta = 0.05$ for $ma = 0.05$ and $\Delta\beta = 0.11$ for $ma = 0.025$. The substantial discrepancy with the last value might point to a large ratio of Λ parameters, which one would not expect in perturbation theory. On the other hand, the quark mass dependence of the critical β does go in the right direction. Thus, the point ($n_f=0.1, ma=0.05$) seems to be very close to the pure SU(3) limit, with the

fermionic sector almost inactive. By contrast, the fermions have very substantial effects when the mass reaches $ma=0.025$; as we have seen, the fermion dynamics completely dominates for $ma=0.01$. The transition from the perturbative, glue-dominated regime to the essentially nonperturbative quark-dominated regime is surprisingly abrupt, however. It may be that a smoother transition to the quenched limit would be seen if the critical values of β could be determined more accurately in future simulations.

$$n_f=1$$

The effective model of Ref. 8 does not predict any chiral-restoration transition for $n_f=1$ due to the presence of the $U_A(1)$ anomaly (even if its magnitude is small due to finite-temperature instanton suppression). We have, therefore, investigated three low values of the quark mass: $ma=0.05$, 0.025 , and 0.0125 . The ranges of possible metastability on the 4^4 lattice were $5.46 \leq \beta \leq 5.50$, $5.44 \leq \beta \leq 5.52$, and $5.42 \leq \beta \leq 5.48$, respectively.

As we see in Fig. 7, there is a clear metastability signal on the $8^3 \times 4$ lattice for $ma=0.05, \beta=5.48$. On the other hand, we did not find any such two-state signals at any point in the transition ranges for the two lower masses (typical examples are shown in Figs. 8 and 9). These results suggest that there is a first-order transition for $ma=0.05$ but not for $ma=0.025$ and 0.0125 .

It is interesting, at this point, to compare our results with those obtained by Fukugita and Ukawa,¹⁸ the only other group to have investigated the case $n_f=1$. These authors studied the order of the transition for $ma=0.05$, 0.1 , 0.2 , and 0.4 . They used a second-order Langevin algorithm to remove the integrable $O(\epsilon)$ terms in Eq. (15) and ran with a step size of $\epsilon=0.02$. They find first-order transitions for all above-mentioned values of the quark mass. They claim that the strength of the transition in-

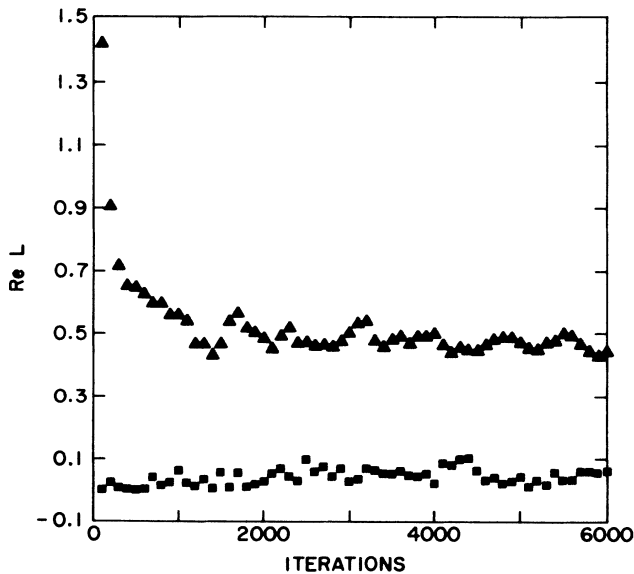


FIG. 7. Same as Fig. 3, but for $n_f=1$, $ma=0.05$, $\beta=5.48$.

creases with the mass. Their critical β for $ma=0.05$, quoted¹⁸ as 5.475 ± 0.005 , agrees well with our result for this mass. This is reassuring, since the systematic errors should be similar (see Sec. II).

A natural interpretation of all these results is, again, as sketched in Fig. 6: a first-order line extends from $(n_f=1, m=\infty)$ down till $(n_f=1, m=m_D)$ where $0.05 < m_D a < 0.025$. The transitions along this line should be caused by gauge field dynamics (the deconfinement phenomenon). The absence of first-order transitions below m_D , together with the prediction of the effective model,⁸ points towards the conclusion that the

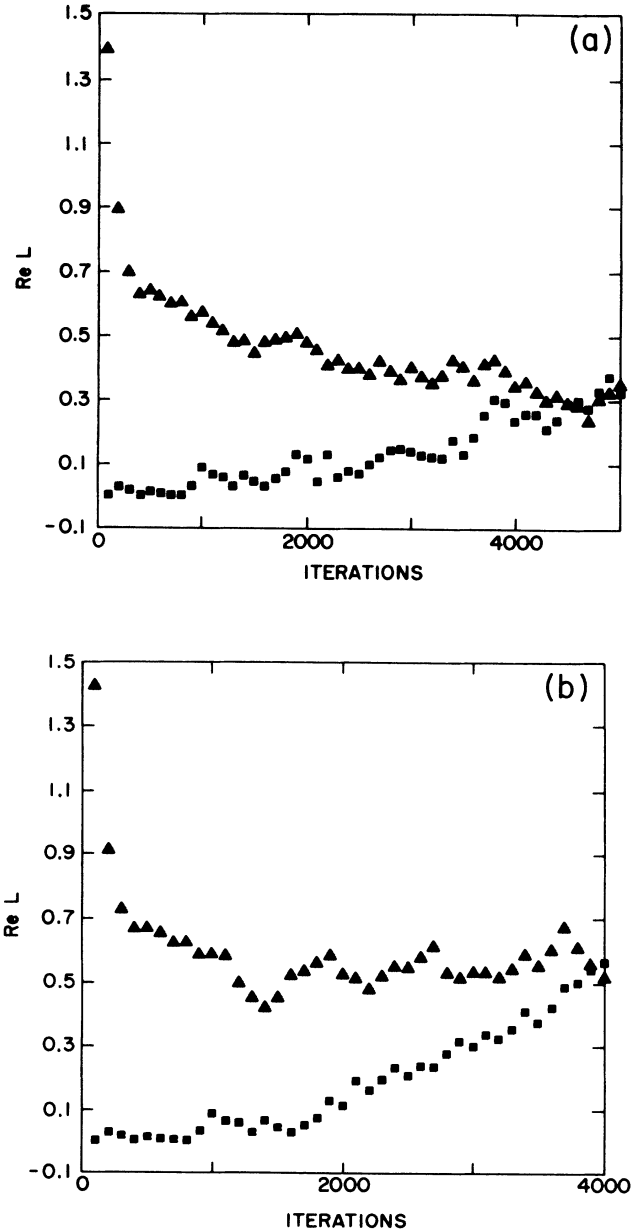


FIG. 8. (a) Same as Fig. 7, but for $n_f=1$, $ma=0.025$, $\beta=5.47$. (b) Same as (a), but for $\beta=5.50$.

dynamical mechanism of chiral-symmetry restoration does not operate for this value of n_f . These conclusions are qualitatively the same as in the case $n_f=0.1$; the main difference is that the end point m_D is larger for $n_f=1$. This is, of course, what one would expect in the spin system analogy for the deconfinement transition.

Although the above interpretations are very appealing since they explain and tie together all known quenched and unquenched numerical results with the predictions of the effective models of Refs. 2 and 8, it is clear that they are subject to the usual caveats of numerical lattice results. Thus, a chiral first-order transition might be found by going to still lower masses, or the whole picture might

be altered as one approaches the continuum limit by using larger lattices. Since one does not know how to perform exact simulations with $n_f=1$ or 0.1 , there is no way of making sure that the systematic errors do not take us out of the universality class of QCD. Finally, the trick we use in order to simulate arbitrary n_f may not be legitimate, especially for $n_f=0.1$.

$$n_f=2$$

This case is physically much more interesting than the previous two, especially if the transition temperature in full QCD is comparable to or less than the current mass of the strange quark (as seems to be indicated by present estimates²³). In that case only the u and d quarks will contribute significantly to the dynamics, and simulations with $n_f=2$ species of mass-degenerate light quarks will not be far from the physical world. On the theoretical side too, the case $n_f=2$ is of special interest. As seen in Table I, the prediction of the effective model of the chiral transition depends on whether the $U_A(1)$ anomaly is sufficiently suppressed at the critical temperature to allow the transition to be first order. Turning the argument around, if we do find a first-order chiral transition for $n_f=2$ and light quark masses, this would imply that $U_A(1)$ symmetry is in fact approximately restored in the high-temperature phase of QCD. Such restoration can lead to dramatic effects in the real world: for instance, the η' - π mass difference should then be much smaller at high temperature than at zero temperature. In view of the prescription for simulating flavor numbers which are not multiples of 4 by means of staggered fermions (see Sec. II), $n_f=2$ is also of great importance. In particular, it is not clear whether the effects of the anomaly can be adequately reproduced by this procedure. Thus, we might in principle find the chiral transition to be first-order on small lattices (with the transition β at intermediate or strong coupling) only to see it become second order on larger lattices (with the transition deep in the scaling region). This would happen if the strength of the anomaly were underestimated at intermediate coupling, with its true value only restored deep in the continuum limit.

We ran our simulations for $ma=0.025$ and 0.1 on $8^3 \times 4$ and 4^4 lattices, and for mass $ma=0.2$ on a 4^4 lattice only. Preliminary runs on the 4^4 lattice ruled out any metastabilities in the case $m=0.2$; the ranges of possible metastability were $5.37 \leq \beta \leq 5.38$ for $ma=0.1$ and $5.3 \leq \beta \leq 5.4$ for $ma=0.025$. On the $8^3 \times 4$ lattice, we found clear metastability signals for $\beta=5.33$ at $ma=0.025$ but none for $ma=0.1$ (all these results are illustrated in Ref. 10).

The case $n_f=2$ has also been studied by other groups. Gottlieb *et al.*¹⁹ simulated $ma=0.025, 0.05, 0.1$. Fukugita and Ukawa¹⁸ used $ma=0.05, 0.1, 0.2, 0.4$, and 1.0 . Kogut and Sinclair²⁰ looked at the case $ma=0.0125$. Gupta *et al.* (last paper in Ref. 21) have used their algorithm on a 4^4 lattice for $ma=0.02$. Because of the use of different simulation algorithms and methods of analysis,¹⁰ there are some quantitative disagreements between these results (for instance, for $ma=0.025$, Ref. 19 finds $\beta_c=5.285$ as compared to our value $\beta_c=5.33$). Nevertheless, quali-

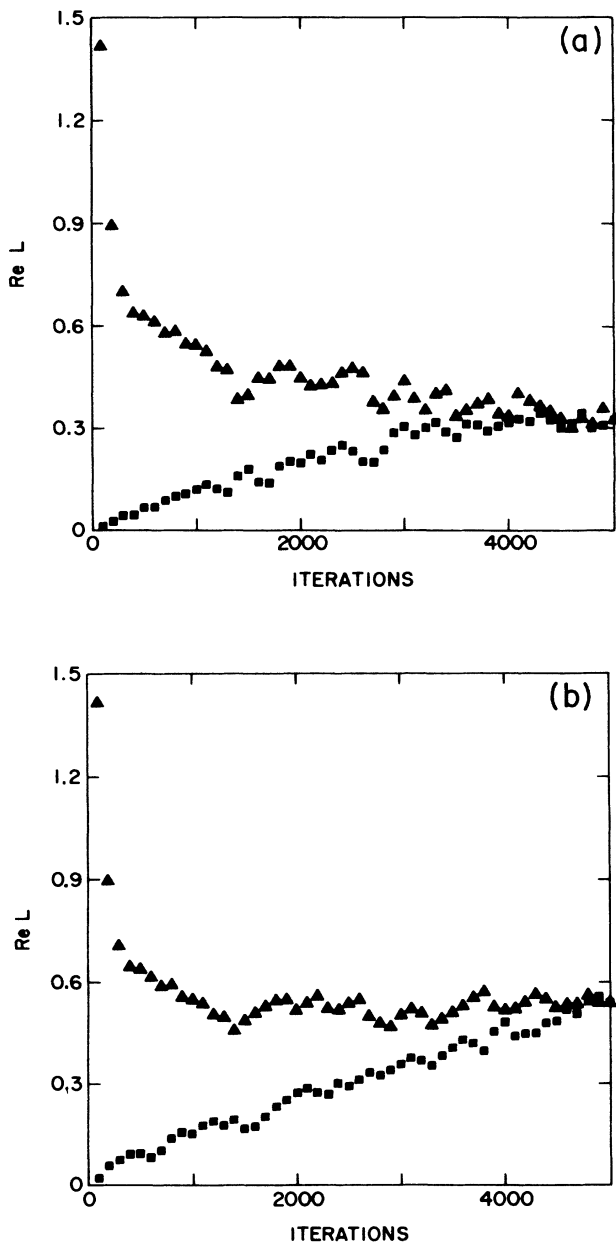


FIG. 9. (a) Same as Fig. 8(a), but for $n_f=1$, $ma=0.0125$, $\beta=5.45$. (b) Same as (a), but for $\beta=5.47$.

tatively it is possible to sum up all of them as in Fig. 6. For $n_f=2$, this features two lines of first-order phase transitions. As in the cases $n_f=0.1$ and 1, a deconfinement line extends from $m = \infty$ down to some $m_D a$ which appears to be larger than 0.2. Again, m_D appears to increase with n_f . As opposed to the situation for lower flavor number, there is now a line of first-order chiral transitions with end point m_{ch} . The main quantitative discrepancy between various studies concerns the value of $m_{ch}a$: Refs. 10 and 19–21 would place it at $m_{ch}a \simeq 0.025$, while Ref. 18 maintains that $m_{ch}a \simeq 0.1$. As we discuss in Ref. 10, we find the latter claim unlikely; a much better understanding of simulation algorithms and methods of analysis is required before a quantitative consensus can be established.

The low-mass transitions are most naturally interpreted as being caused by the chiral-symmetry-restoration mechanism of massless QCD, described by the effective model of Ref. 8. The simultaneous jump in other variables such as the deconfinement order parameter could be explained as an induced phenomenon: once a first-order phase transition takes place, *all* observables will show discontinuities. In this sense, the chiral line is dual to the deconfinement line, on which the jump in the Polyakov loop reflects the underlying physics of the transition while the jump in the chiral condensate is merely induced. Note also that, using the current estimates of the transition temperature in QCD, the light isodoublet mass in the real world should correspond to $ma \approx 0.012$ (Ref. 11). This would predict a first-order chiral-restoration transition in QCD, accompanied by a partial restoration of axial U(1) symmetry.

As we discussed above, the use of the fractional-flavor scheme casts some doubt on the relevance of all these results to the physical continuum limit. One way to make sure that the first-order transitions are genuine is to repeat the simulations on larger lattices (longer in the temperature direction as well). It is also very interesting to see how the gap between the end points $m_{ch}a$ and $m_D a$ behaves as the lattice expands; if the gap narrows, it might indicate that the region of analyticity in the critical surface is merely a lattice artifact; if it expands, the real-world value of ma might come uncomfortably close to the gap.

$$2 < n_f \leq 3$$

The case $n_f=3$, $ma=0.1$ had been investigated by two groups prior to the current generation of supercomputer simulations of full QCD (Ref. 24). While there was a disagreement about the order of the transition, it seems fair to say that the data of both were consistent with a continuous or at best a weakly first-order phase transition. By contrast, our simulations reported in Refs. 9 and 11 show evidence of a strong first-order transition when the mass is lowered to $ma=0.025$. Reference 11 also reports the results of simulations performed with a dynamical isodoublet of mass 0.025 and with a dynamical “strange” quark whose mass in lattice units is $R \times 0.025$. By varying R , we interpolate between $n_f=2$ ($R = \infty$) and $n_f=3$ ($R=1$). We find first-order phase transitions for

all values of R , with the transition β decreasing from ≈ 5.33 for $n_f=2$ to ≈ 5.1 for $n_f=3$.

The effective model of chiral restoration predicts a strong first-order transition for $n_f=3$, irrespective of the anomaly.⁸ Also, in the magnetic-field analogy for that model, the end point m_{ch} should increase as the number of flavors increases. These considerations would lead us to ascribe the first-order transitions we observed for $ma=0.025$ to the chiral mechanism, with $m_{ch}a \simeq 0.1$. It seems reasonable to assume the existence of a first-order line of deconfinement transitions for higher mass values. It will be interesting to search for this line in the case $n_f=3$.

$$n_f \geq 4$$

As we mentioned above, our algorithm and methods of analysis were first tested against the results of Ref. 7 for the case $n_f=4, ma=0.025$ on a 4^4 lattice.⁹ We agreed with the conclusion of Ref. 7 that a first-order chiral transition occurs with those parameter values, but our value of $\beta_c \approx 5.03$ was larger than theirs. The existence of a first-order transition was also confirmed by all the other groups who studied this combination of flavor number and quark mass.¹⁸ The first-order chiral line at $n_f=4$ in Fig. 6 represents this consensus. Different systematic errors due to different algorithms were seen to lead to shifts in the critical coupling, while being unable to obscure the order of this very strong first-order transition.

On the other hand, the existence and location of the end points m_{ch} and m_D remain controversial.^{18,21} Gupta *et al.* are the only group to maintain that the phase transition remains first order up to $ma=0.5$. Thus, they argue, there might be no gap between the chiral and the deconfinement line, at least not for $n_f=4$. All the other groups who have studied masses larger than 0.025 do see a gap, but the exact values of m_{ch} and m_D are not clear (it would seem that $m_{ch}a \sim 0.1$; $m_D a \sim 0.4$). As we have discussed above, our simulations for $n_f < 4$ certainly suggest the existence of a gap between the chiral and the deconfinement lines.

For completeness, let us also mention that results obtained by other authors shed light on what happens to the phase diagram for large flavor number.^{18,25} The first-order chiral transition appears to become stronger and to expand rapidly towards higher masses. For $n_f \geq 10$, it is claimed that the gap has been already closed by the expansion of the chiral line. A finite-temperature first-order transition has been reported for $n_f=18$, where it must necessarily be due to the chiral mechanism since the theory should always be in its confining phase. These results were used in completing Fig. 6.

IV. CONCLUSIONS

Using a shifted first-order Langevin algorithm, we have investigated the phase diagram of finite-temperature QCD and 4^4 and $8^3 \times 4$ lattices with 0.1, 1, 2, 3, and 4 quark flavors of mass between 0.01 and 0.05 in lattice units. As with any algorithm based on the numerical integration of discretized differential equations, our results,

obtained for a step size of $\epsilon=0.01$, would have to be extrapolated to $\epsilon=0$ in order to become quantitatively reliable. Nevertheless, our qualitative conclusions agree well with the predictions of effective theories as well as with other simulations. In particular, we can reproduce the order of the phase transition observed for $n_f=4$, $ma=0.025$ with an algorithm⁷ which is free of finite step-size errors. This comparison appears to vindicate our initial hypothesis, that the step size we chose is small enough to keep our simulations within the universality class of QCD even for the smallest masses we studied. We have shown by direct tests that the other unphysical simulation parameter, namely, the fermion matrix inversion residue r of Eq. (20), lies in a range where the results on the order of the transition are independent of r .

Table II summarizes the values of the critical couplings at which we found evidence for metastability at various values of n_f and ma . The comparison with the results of other simulations shows that these values are affected by systematic errors due to the finite step size: they tend to be too large by a few percent. However, the qualitative trends are as expected; β_c decreases as n_f is increased and as the quark mass is lowered. The difference between the critical coupling for the quenched theory and the value of β_c we obtain for $n_f=0.1$ is in agreement with the perturbative renormalization-group prediction for $ma=0.05$ but not for lighter masses. The importance of nonperturbative fermionic effects so close to the quenched limit $n_f=0$ is surprising.

We have entered our results on the order of the phase transitions for various flavor numbers and quark masses into Fig. 6, together with relevant results obtained by other groups. The picture which emerges is consistent with the expectations based on the study of effective models.^{2,8} There are two sets of lines of first-order phase transitions: one set which reaches down from $m=\infty$ to some end point $m_D(n_f)$ and one which extends upwards from $m=0$ to some $m_{\text{ch}}(n_f)$. We have been led to interpret the first set as due to the deconfinement mechanism in the pure-gluon sector of the theory. This mechanism should be active for all $n_f < \frac{33}{2}$; our simulations confirm that m_D decreases with the number of flavors. It is presumably also the cause of the transitions previously seen in the quenched approximation, which is realized along the lines at $m=\infty$ and $n_f=0$. We interpreted the jump in the chiral order parameter which accompanies the deconfinement transition as induced by the strong first-order character of this transition.

On the other hand, we have taken the connection of

TABLE II. Summary of β_c as a function of n_f and ma for first-order phase transitions we detected on $8^3 \times 4$ lattices. No entry indicates the absence of evidence for metastability. The value for $ma=\infty$ is taken from Ref. 18.

$n_f \backslash ma$	0.025	0.05	0.1	∞
0.1	5.58	5.64	Not done	5.675
1		5.48	Not done	5.675
2	5.33			5.675
3	5.1			5.675

the second set of lines to the massless (chiral) limit of the theory as an indication that these transitions must be due to the chiral-symmetry-restoration mechanism described in Ref. 8. In this interpretation, the simultaneous jump in the Polyakov loop must be induced by the interaction of the fermionic and gauge sectors. The n_f dependence predicted by this effective model is confirmed by our results. For the two-flavor case, where the prediction depended on the strength of the finite-temperature anomaly, we find that the transition appears to be first order. The end point $m_{\text{ch}}(n_f)$ appears to increase with the number of flavors. Fukugita and Ukawa¹⁸ claim that this growth is so rapid, that it closes the gap between the two lines of first-order transitions for $n_f \geq 10$.

Our simulation results definitely favor the existence of this gap, at least in the region of low quark masses and small n_f . Coming back to the three-dimensional phase diagram sketched in Fig. 2, the simplest assumption would be that the deconfinement transition in full QCD occurs at the same physical temperature $T_D = T_{\text{SU}(3)}$ as in pure SU(3) theory, while the chiral transition takes place at the temperature $T_{\text{ch}} = T_{\text{QCD}}$ which was preliminarily measured for $n_f=2$ in Ref. 23. This would lead to a picture consisting of two disconnected half-planes of first-order transitions, one at $T=T_D$ and one at the lower temperature T_{ch} . Alternatively, there might be a single critical surface with nonzero curvature, of equation $T_c = F(n_f, m)$. The absence of first-order transitions for certain m, n_f would manifest itself as a hole in this curved surface. So far, the critical temperature has been measured in the quenched limit and (preliminarily) for $n_f=2$ and low masses; it would have to be measured for various combinations of flavor number and quark mass in order to yield information about the shape of the critical surface.

To the extent that our findings agree with the expectations based on effective models and present a certain consistency with each other and with other simulations, they offer an *a posteriori* justification for the flavor simulation prescription we used. This is true at least for the purely thermodynamical aspects of the theory. A much more difficult and subtle question is whether the prescription is able to reproduce the physical effects of the anomaly at the couplings where the transition takes place. In particular, is the chiral transition for two flavors really first order? While pioneering studies of the topological susceptibility in pure SU(3) theory seem to confirm that the anomaly is suppressed at the critical temperature,²⁶ it is not clear how this effect can be seen with the staggered fermion recipe we are using. A straightforward way to address this is to verify that the chiral transition remains first order as the number of sites in the time direction is increased, thereby pushing β_c towards the scaling region.

Scaling studies consisting essentially of a repetition of the present work on larger lattices are also necessary in order to see whether the analyticity gap between $m_D(n_f)$ and $m_{\text{ch}}(n_f)$ can survive the passage to the continuum limit. If the end points scale with the lattice, the gap in the critical surface must be physical. If the ratio between the light isodoublet mass and m_{ch} also scales, the conclusion that real-world QCD is characterized by a first-

order chiral transition will be greatly strengthened.

To sum up, our present knowledge of the phase diagram of QCD at finite temperatures, obtained from lattice simulations and from effective model studies, favors the existence of a first-order QCD transition in the real world. This should be accompanied by a partial restoration of axial U(1) symmetry, that is, the $\eta' - \pi$ mass difference in the QCD "plasma" phase should be much smaller than in the hadronic phase. There also appears to be a region in the phase diagram where the two phases are *not* separated by first-order transitions. This would indicate that part of the physical excitations in the "plasma" phase are (parity-doubled) color-singlet hadrons.²⁷ All of these conclusions must be tested against simulations on larger lattices, with faster and more reliable algorithms and methods of analysis.

Note added. After completion of this manuscript, we received two papers which report pioneering studies of the deconfinement transition in pure SU(3) theory on lattices which are very large by previous standards:

$48 \times 10^2 \times 4$ (Ref. 28) and $16^3 \times 4$ and $24^3 \times 4$ (Ref. 29). Their results seem to suggest that the first-order character of the transition weakens as the spatial size of the lattice increases. Interestingly, these results seem to be in better agreement with the behavior of the effective theory of deconfinement^{2,30} than previous simulations on smaller lattices. While such findings will have to be confirmed and made precise by more detailed studies, they dramatize the role finite-volume effects could play in judging the order of a phase transition from lattice studies.

ACKNOWLEDGMENTS

The computations necessary for this work were carried out on the Cray X-MP/22 at the National Magnetic Fusion Energy Computing Center at Lawrence Livermore National Laboratory. This work was partially supported by the U.S. Department of Energy under Contract No. DE-AC02-76CH00016.

-
- ¹J. Kogut, M. Stone, H. W. Wyld, W. R. Gibbs, J. Shigemitsu, S. H. Shenker, and D. K. Sinclair, *Phys. Rev. Lett.* **50**, 393 (1983).
- ²See, e.g., B. Svetitsky, *Phys. Rep.* **132**, 1 (1986), and references therein.
- ³See, e.g., J. Cleymans, R. V. Gvai, and E. Suhonen, *Phys. Rep.* **130**, 217 (1986), and references therein.
- ⁴T. Banks and A. Ukawa, *Nucl. Phys.* **B225** [FS9], 145 (1983); T. DeGrand and C. DeTar, *ibid.* **B225** [FS9], 590 (1983).
- ⁵P. Hasenfratz, F. Karsch, and H. Satz, *Phys. Lett.* **133B**, 221 (1983).
- ⁶N. Attig, R. V. Gvai, B. Petersson, and M. Wolff, *Z. Phys. C* (to be published).
- ⁷R. Gupta, G. Guralnik, G. W. Kilcup, A. Patel, and S. R. Sharpe, *Phys. Rev. Lett.* **57**, 2621 (1986).
- ⁸R. D. Pisarski and F. Wilczek, *Phys. Rev. D* **29**, 338 (1984); H. Gausterer and S. Sanielevici, Report No. BNL-41212, 1988 (unpublished); *Phys. Lett. B* (to be published). For the special case $n_f = 3$, see also H. Goldberg, *Phys. Lett.* **131B**, 133 (1983); A. Margaritis and A. Patkos, *Phys. Lett. B* **178**, 272 (1986).
- ⁹R. V. Gvai, J. Potvin, and S. Sanielevici, *Phys. Rev. Lett.* **58**, 2519 (1987).
- ¹⁰R. V. Gvai, J. Potvin, and S. Sanielevici, *Phys. Lett. B* **200**, 137 (1988).
- ¹¹R. V. Gvai, J. Potvin, and S. Sanielevici, *Phys. Rev. D* **37**, 1343 (1988).
- ¹²See, e.g., H. Kluberg-Stern, A. Morel, O. Napoly, and B. Petersson, *Nucl. Phys.* **B190** [FS3], 504 (1981).
- ¹³A. Billoire, R. Lacaze, E. Marinari, and A. Morel, *Nucl. Phys.* **B251** [FS13], 581 (1985).
- ¹⁴H. W. Hamber, E. Marinari, G. Parisi, and C. Rebbi, *Phys. Lett.* **124B**, 99 (1983).
- ¹⁵A. Ukawa and M. Fukugita, *Phys. Rev. Lett.* **55**, 1854 (1985); G. G. Batrouni, G. R. Katz, A. S. Kronfeld, G. P. Lepage, B. Svetitsky, and K. G. Wilson, *Phys. Rev. D* **32**, 2736 (1985); G. G. Batrouni, *ibid.* **33**, 1815 (1986); A. S. Kronfeld, *Phys. Lett. B* **172**, 93 (1986).
- ¹⁶R. V. Gvai, J. Potvin, and S. Sanielevici, *Phys. Rev. D* **36**, 1912 (1987); *Phys. Lett. B* **183**, 86 (1987).
- ¹⁷R. V. Gvai, A. Gocksch, and U. Heller, *Nucl. Phys.* **B283**, 281 (1987).
- ¹⁸M. Fukugita, *Nucl. Phys. B (Proc. Suppl.)* **4**, 105 (1988); M. Fukugita and A. Ukawa, *Phys. Rev. D* **38**, 1971 (1988).
- ¹⁹S. Gottlieb, W. Liu, D. Toussaint, R. L. Renken, and R. L. Sugar, *Phys. Rev. D* **35**, 3972 (1987).
- ²⁰J. B. Kogut and D. K. Sinclair, Report No. ILL-(TH)-87-46, 1987 (unpublished).
- ²¹R. Gupta, *Nucl. Phys. B (Proc. Suppl.)* **4**, 562 (1988); R. Gupta, G. W. Kilcup, and S. R. Sharpe, *Phys. Rev. D* **38**, 1288 (1988); R. Gupta, G. Guralnik, G. W. Kilcup, A. Patel, and S. R. Sharpe, *Phys. Lett. B* **201**, 503 (1988).
- ²²A. D. Kennedy, J. Kuti, S. Meyer, and B. J. Pendleton, *Phys. Rev. Lett.* **55**, 1958 (1985). For measurements on larger lattices, see S. Gottlieb, A. D. Kennedy, J. Kuti, S. Meyer, B. J. Pendleton, R. L. Sugar, and D. Toussaint, *ibid.* **55**, 1958 (1985); N. H. Christ and A. E. Terrano, *ibid.* **56**, 111 (1986).
- ²³S. Gottlieb, W. Liu, R. L. Renken, R. L. Sugar, and D. Toussaint, *Phys. Rev. Lett.* **59**, 1513 (1987); M. Fukugita, S. Ohta, Y. Oyanagi, and A. Ukawa, *ibid.* **58**, 2515 (1987).
- ²⁴R. V. Gvai and F. Karsch, *Nucl. Phys.* **B261**, 273 (1985); F. Fucito and S. Solomon, *Phys. Rev. Lett.* **55**, 2641 (1985).
- ²⁵N. Attig, B. Petersson, and M. Wolff, *Phys. Lett. B* **190**, 143 (1987).
- ²⁶J. Hoek, M. Teper, and J. Waterhouse, *Phys. Lett. B* **180**, 112 (1986).
- ²⁷C. DeTar, *Phys. Rev. D* **32**, 276 (1985); T. A. DeGrand and C. DeTar, *ibid.* **34**, 2469 (1986); C. DeTar and J. Kogut, *Phys. Rev. Lett.* **59**, 399 (1987); *Phys. Rev. D* **36**, 2828 (1987). For the usual "plasma" picture see, e.g., L. McLerran, *Rev. Mod. Phys.* **58**, 1021 (1986).
- ²⁸APE Collaboration, P. Bacilieri *et al.*, *Phys. Rev. Lett.* **61**, 1545 (1988).
- ²⁹F. R. Brown, N. H. Christ, Y. Deng, M. Gao, and T. J. Woch, Columbia Report No. CU-TP-407, 1988 (unpublished).
- ³⁰H. W. J. Blöte and R. H. Swendsen, *Phys. Rev. Lett.* **43**, 799 (1979); H. J. Herrmann, *Z. Phys. B* **35**, 171 (1979); S. J. Knak Jansen and O. G. Mouritsen, *Phys. Rev. Lett.* **43**, 1736 (1979).